

Design and Characteristics Analysis of a Novel Single-phase Hybrid SRM for Blender Application

Kwang-II Jeong* and Jin-Woo Ahn[†]

Abstract – In this paper, the design and characteristic analysis of a novel single-phase hybrid switched reluctance motor (HSRM) for the purpose of replacing the universal motor in commercial blenders are presented. The proposed motor is easy to manufacture due to its simple yet robust structure with minimized power switches and no torque dead-zone. Moreover, the proposed HSRM is able to deliver a high starting torque as a requirement for blending hard food or even ice. The stator has permanent magnets (PMs) mounted on its inner surface and the rotor has a wide pole arc and salient poles that contribute to its high starting torque profile and the elimination of the torque dead-zone. Finite element method (FEM) is used to analyze the characteristic of the proposed motor. Finally, the prototype is manufactured and its performance is verified through experiments.

Keywords: Single-phase HSRM, Permanent magnet, Blender, Salient poles, Torque dead-zone, Non-uniform air-gap

1. Introduction

The history of electrical drive goes back to 1838 and it has been inseparable from human lives since Electric motors are commonly found nowadays in a wide range of household or industrial applications, such as vacuum cleaners, pumps, compressors, and hammer drills. Among a variation of motor types, there is one type that is quite popular for commercial applications: universal motors. As the name suggests, universal motors work with either AC or DC power supply and it has a simple structure. Moreover, no special converter is required, so weight and cost of the drive can be reduced, which is an important factor in industry and business. However, universal motors suffer from problems as listed below:

- Short lifespan due to the wear of carbon brushes and commutator (regular maintenance is needed)
- High sensitivity to moisture and dust especially if it is electrically conductive. Applications in extreme environment may require an extra cost for protection.
- ‘Limited’ power to weight ratio. The possible speed range is limited due to the commutator and rotor windings. The motor can run above the rated speed, but at the expense of significantly reduced commutator lifespan.
- Moderate dynamic characteristics, mainly due to the high rotor inertia. Although high acceleration is seldom needed, rapid braking is a requirement for some applications. The motor is able to brake, but it needs

additional switchgear (a reversing switch for either stator or rotor windings). For a controlled braking operation, a supplementary electronic control is necessary, which adds to the cost.

Fig. 1 shows the structure of blender with a universal motor. As can be seen in the figure, the brush is located near the impeller which increases the potential of carbon dust exposure to its surroundings. In addition, if somehow high load occurs during blending process, the speed rapidly decreases, which lowers the efficiency.

Therefore, it is considered necessary to replace universal motors with another type that is competitive in cost, but has better performance, such as high efficiency at full load.

Brushless motors certainly do not have these drawbacks that are caused by the commutator or brush. However, their control electronics are usually costly. The comparison of brushless motor types is given in Fig. 2. The main cost influencing factors are: the number of turns in the winding, the winding construction and manufacturing method, the amount and quality of permanent magnets, the number and

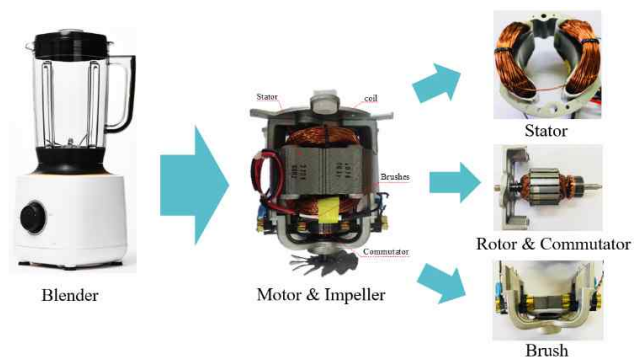


Fig. 1. Structure of blender

[†] Corresponding Author: Dept. of Mechatronics Engineering, Kyungshung University, Korea. (jwahn@ks.ac.kr)

* Dept. of Mechatronics Engineering, Kyungshung University, Korea. (you486-7179@hanmail.net)

Received: April 5, 2018; Accepted: May 12, 2018

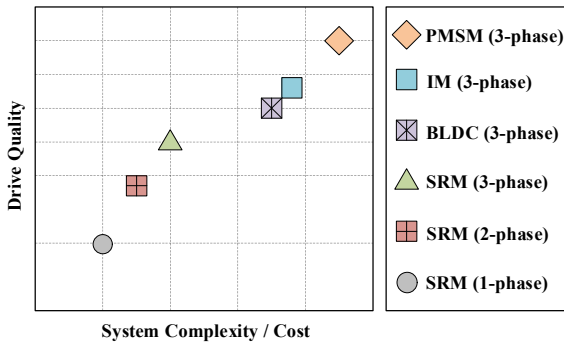


Fig. 2. Quality and complexity of brushless drives

size of semiconductors in the inverter bridge, and the complexity of the control algorithm and the number of required sensors (speed, position, current). In this regard, poly-phase drives may be considered more complex than two- or single-phase ones. Motors using costly magnets or distributed windings, like PM-synchronous or brushless-DC, are probably more expensive than the motors without, like induction or switched reluctance motors.

Switched reluctance motor (SRM) is a doubly salient and singly excited motor, in which windings are located on the stator and no windings or permanent magnets (PMs) are located on the rotor. The motor structure has many merits, such as good fault tolerance, robustness, low cost and applicability in harsh environments, such as high speed or high temperature [1-4]. To compete with the low cost universal motor, an effective way is by reducing the number of switches in converter which means choosing unipolar drives over bipolar drives. Single-phase SRMs suit the unipolar excitations by nature and have been involved in many studies as an effective low cost drive system [5, 6]. However, a lot of research only focus on reducing the converter's cost instead of the motor's. For example, a single-controllable-switch converter was proposed in [7] for controlling an asymmetric two-phase SR motor, and a modified topology was proposed in [8] with improved current controllability. There is no doubt that in order to achieve a good low-cost solution, it is important that the converter, the motor control, and the motor design should be researched together.

A single-phase type SRM and its corresponding converter will have both the simplest structure and the lowest cost to produce among other SRM designs. However, for conventional single-phase SRMs, there is a dead torque zone occupying half of one electrical period, which results in high torque ripple. Moreover, the initial positioning to enable self-start of a single phase SR machine is also a problem. Often, parking magnets or parking windings are used in single-phase SR machines to hold the rotor at a proper initial starting position [9].

In this paper, a novel single-phase hybrid switched reluctance motor (HSRM) for blender application which uses both the reluctance flux and permanent magnet interaction together to generate torque is presented. The

cogging torque produced from permanent magnets is properly utilized to reduce the torque ripple. Also, the self-starting capability and high starting torque is made possible by the non-uniform air-gap with a percentage of pole saliency on each side of rotor. Experiments were done to verify the performance of the proposed hybrid switched reluctance motor.

2. Structure of Proposed Single-Phase SRM

2.1 Conventional hybrid SRM

The structure of conventional 4/4 HSRM is shown in Fig. 3. There are four poles for each rotor and stator, two permanent magnets mounted on the inner surface of the stator. The rotor surface is smooth and provides uniform air-gap between rotor and stator.

The electromagnetic energy conversion happens in the air-gap. Therefore, the flux in the air-gap is important since it determines the output profile of the motor. Thus, correctly modifying the air-gap may improve the output. This paper focuses on modifying the rotor pole to change the air-gap in order to improve output. Fig. 4 below shows the rotor pole of the conventional type. The rotor pole arc, β_r , is the main parameter to be modified.

There are two kinds of flux-linkage in a hybrid SRM:

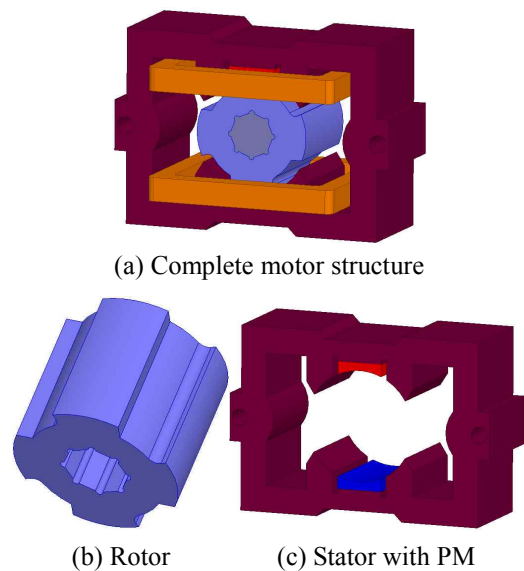


Fig. 3. 3D model of conventional hybrid SRM

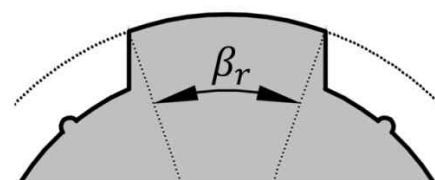


Fig. 4. Conventional rotor pole

flux due to the permanent magnets (f_{PM}) and flux due to winding excitation (f_w). Since the permanent magnets are mounted on the stator permanently, the existence of PM flux cannot be eliminated, thus affecting the generation of f_w . However, the analysis of each flux is made possible through simulation. Therefore, in this paper, two kinds of flux linkage to be observed are PM flux and total flux or reluctance flux (f_r) which can be described as:

$$f_r = f_{PM} + f_w \quad (1)$$

Flux changes according to the position of rotor pole, as shown in equation 2.

$$\lambda = L(\theta, i) i \quad (2)$$

where λ is the phase flux linkage and $L(\theta, i)$ is the inductance dependent on rotor position θ and phase current i . As the rotor pole is closing in or aligning with a stator pole during phase excitation, the reluctance decreases while the inductance increases, and vice versa. This affects the flux. As previously stated, flux flow changes depending on the rotor position with the aligned one leads to the highest flux being transferred from stator to rotor side.

As can be seen in Fig. 5, due to the uniform air-gap, the increasing and decreasing flux-linkages are symmetric, which is true for any conventional SRM types. This flux affects the output torque of the motor, as explained before. Their relationship is shown in equation 3.

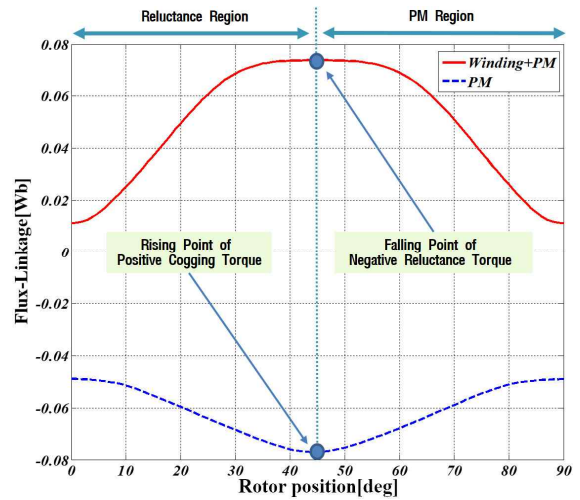
$$T_e = \frac{dL(\theta, i)}{d\theta} \cdot \frac{i^2}{2} \quad (3)$$

where T_e is the electrical torque. T_e changes according to the rate of change of inductance, which means that no torque will be generated if there is no change of inductance. It is common to use inductance profile only to estimate the output torque of an SRM.

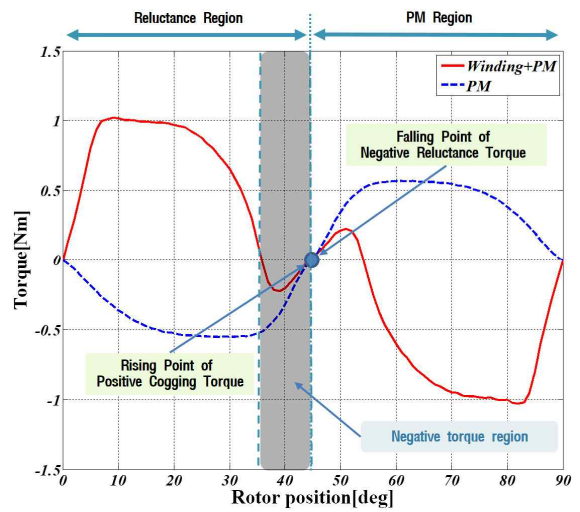
Examining flux-linkage in Fig. 5(a) alone, there is a region where f_r is not changing while f_{PM} is. This causes a negative torque to be generated in that specific region, that interrupts the operation of the motor. Because of this region, the rotation of the rotor is slightly reversed before being pulled forward for normal operation. The generated torque can be seen in Fig. 5(b).

2.2 Non-uniform air-gap

As described before, the output torque can be modified by modifying the air gap as it is where electromagnetic energy conversion happens. Since this paper focuses on the rotor structure, a non-symmetric rotor structure which will create variation in the air gap can be utilized. The detailed design is shown in Fig. 6. Here, β_m is the non-uniform part of the rotor arc meant to modify the inductance and

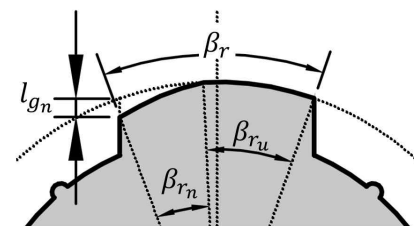


(a) Flux linkage

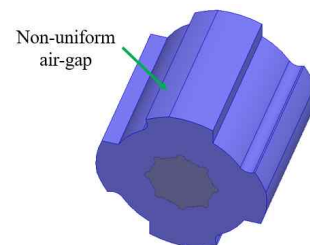


(b) Electrical torque

Fig. 5. Output of conventional HSRM



(a) 2D design of one rotor pole



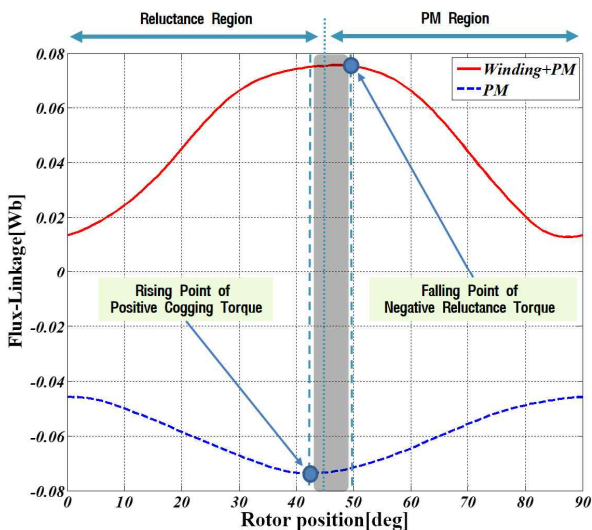
(b) 3D model

Fig. 6. 3D model of hybrid SRM with non-uniform air-gap

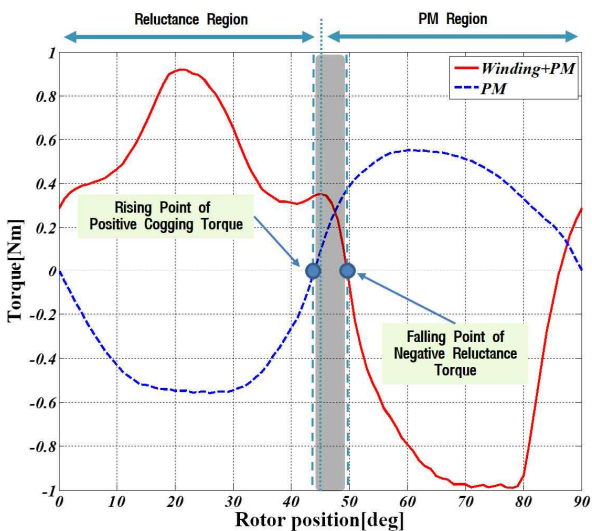
β_{ru} is the uniform part of the rotor arc. The non-uniform air-gap length l_{gn} needs to be carefully selected because if l_{gn} is too large, then negative torque region will be formed. This also applies to the percentage selection of β_{rn} and β_{ru} . By doing this, the “flat part” of the flux as previously shown in Fig. 5(a) can be eliminated. Compared to the conventional design, the decreasing point of f_r and the increasing point of f_{PM} has been shifted to the right and left, accordingly. This eliminates the existing negative torque region in conventional rotor structure. Furthermore, the positive torque area of the non-symmetric rotor structure is much wider. The whole phenomena can be seen in Fig. 7.

2.3 Proposed structure

A blender is an appliance used to mix or puree food.



(a) Flux linkage



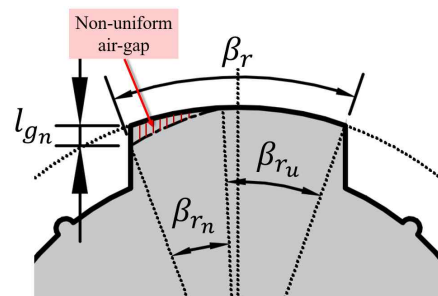
(b) Electrical torque

Fig. 7. Output of HSRM with non-uniform air-gap

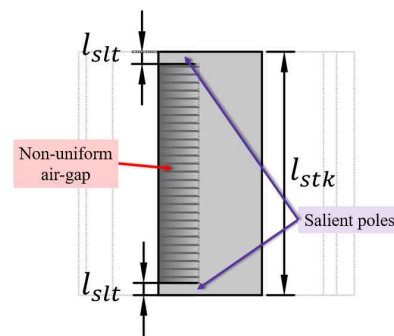
People put different things in blender, starting from a soft substance such as yogurt, to hard substance such as apples or even ice. Therefore, one of the important factors to be considered in designing blender motor drive is its starting torque. The cogging torque produced by PMs is useful to hold the rotor at initial rotating position. Therefore, the starting torque, T_{st} has to be larger than the permanent magnet cogging torque T_{PM} in order to start the rotation. Also, when the excitation is turned off (after poles have been aligned), rotor rotation depends on the cogging torque until rotor pole is aligned with PMs, which is when the excitation sequence begins again.

It was shown before that the negative torque region can be eliminated by utilizing non-uniform air-gap. In order to increase the starting torque, some salient parts of the rotor pole are “saved” in design process, creating a structure shown in Fig. 8. The non-uniform air-gap part still exists, but it looks like it has sunken in the middle.

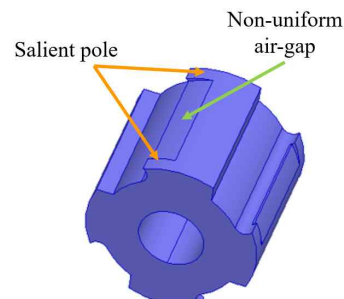
The salient length part l_{slt} is selected accordingly in



(a) 2D design of one rotor pole (front view)



(b) 2D design of one rotor pole (bird view)



(c) 3D model

Fig. 8. 3D model of hybrid SRM with non-uniform air-gap

terms of percentage or ratio to the core stack length l_{stk} . The resulting flux linkage profile can be seen in Fig. 9(a). The decreasing and increasing points of f_r and f_{PM} are shifted as confirmed in the previous subsection. However, by utilizing this structure, the starting torque can be

increased by almost 1.5 times.

2.4 Design Optimization

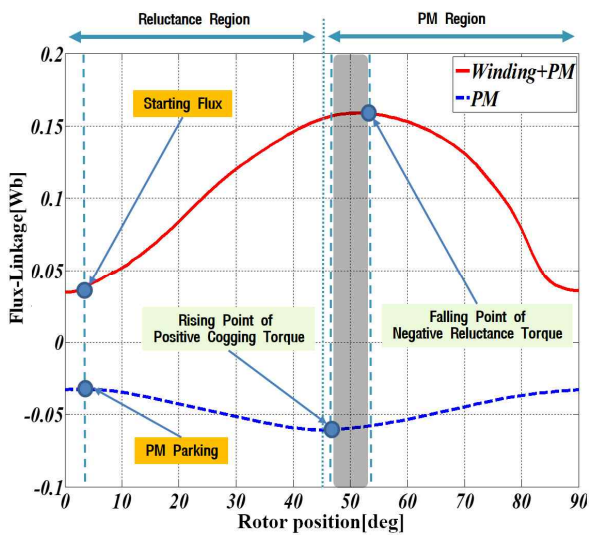
The higher starting torque and lower torque ripple can be acquired by increasing the air gap on a fractional part of the rotor pole arc. Thus, in order to get higher starting torque and lower torque ripple in this structure, air gap modification has to be done. The saliency ratio of l_{sl} and l_{stk} are selected and simulated to find the optimized value. If l_{sl} is too long, then it will eradicate the effect of non-uniform air-gap and if it is too short, then the starting torque cannot be increased as much. Three different air-gaps are modeled as presented in Fig. 10.

However, this salient part does not only increase the starting torque, but it also changes the whole torque profile. The result of this optimization is discussed in the next section.

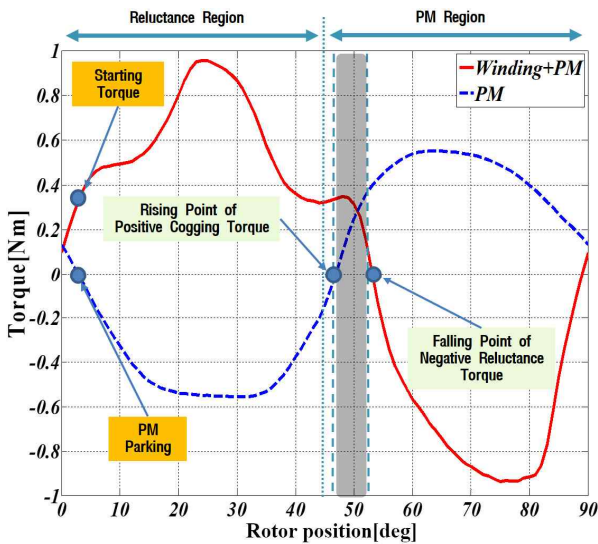
3. Structure of Proposed Single-Phase SRM

3.1 Operating principle

The proposed motor utilizes permanent magnets placed above and below the rotor. It is used to park the rotor, giving it a definite starting position for each operation. Moreover, during operation, the PMs serve to pull the rotor when the phase excitation is turned off. The detailed operation of the proposed motor can be explained as follows. When the rotor is at the parking position, where the rotor poles are aligned by the effect of the two PMs mounted on stator, there is no current flowing in the motor as shown in Fig. 11(a). This is the starting position for each operation cycle. If current is provided to winding terminal, the rotor will be pulled until it is aligned with the stator poles. When the rotor has almost reached the aligned position during this phase excitation, the phase is switched off, as illustrated in Fig. 11(b). However, even though



(a) Flux linkage



(b) Electrical torque

Fig. 9. Output of proposed HSRM

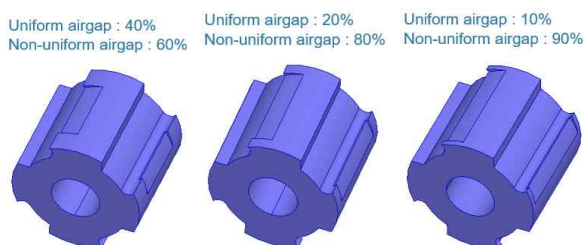
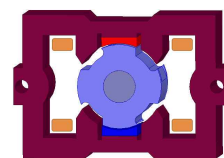
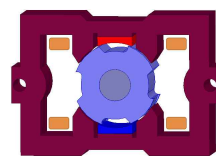


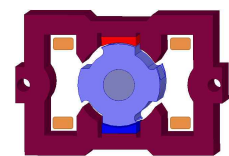
Fig. 10. Three rotor saliency models



(a) Parking position (unaligned position)

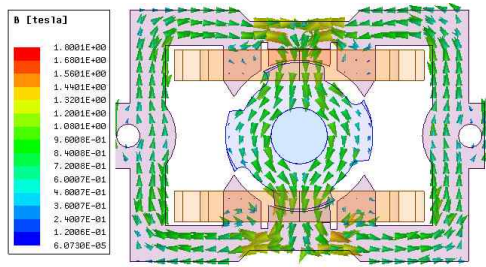


(b) Winding excitation (Aligned position)

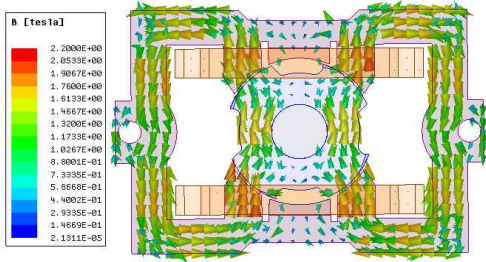


(c) Cogging torque (PM only)

Fig. 11. The working principle of proposed motor



(a) Only PM magnetic flux vector



(a) Winding+PM magnetic flux vector

Fig. 12. Magnetic flux vector of the proposed HSRM

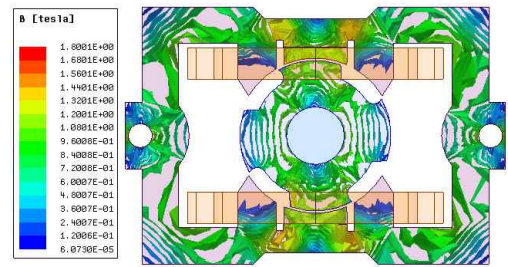
there is no electromagnetic torque generated in the phase windings, the rotor still moves by depending on the momentum and the pulling force of PMs. Then, the rotor is aligned once more with the PMs, as can be seen in Fig. 11(c). To be noted here, this position is the starting position mentioned earlier. By repeating this procedure, a steady state operation can be achieved.

3.2 Magnetic field vector

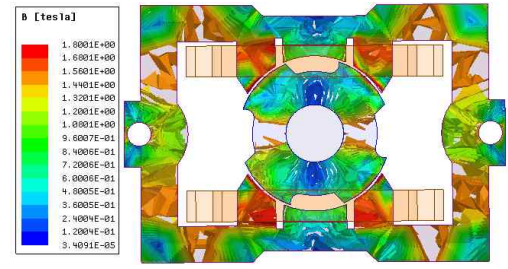
Fig. 12 shows the magnetic field vector of the proposed HSRM at aligned position. Fig. 12(a) shows the f_{PM} provided by permanent magnets at the starting position and Fig. 12(b) shows the flux during phase excitation or f_r . By examining the figures, it can be seen that the flux direction of f_{PM} and f_r differs from each other. This is because f_r has to “win over” f_{PM} to start and maintain the steady rotation of the rotor.

3.3 Magnetic field density

SRM is designed to operate in the saturated region. At the aligned position, maximum inductance is reached and it gets magnetically saturated easily. On the other hand, minimum inductance is reached at unaligned position. As the rotor position affects the saturation, it is necessary to check the magnetic field density when analyzing a motor, especially SRM. Fig. 13 shows the magnetic flux density of the proposed structure at aligned position at rated condition. The material used for stator and rotor cores is 35PN440. Based on simulation result which shows that the maximum flux density is less than 1.8 Tesla, the proposed design satisfies the material requirement.



(a) Only PM magnetic flux density



(a) Winding+PM magnetic flux density

Fig. 13. Magnetic flux density of the proposed HSRM

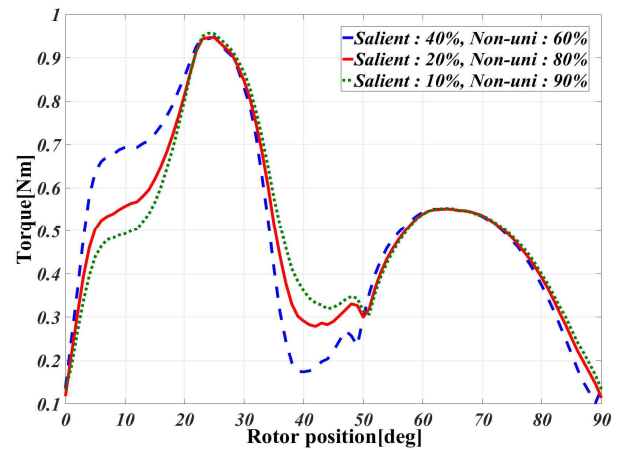


Fig. 14. Torque ripple comparison

3.4 Torque profile

In the previous section, it has been shown that rotor optimization was executed. The addition of saliency to the non-uniform part of the rotor changes the torque profile. Other than increasing the starting torque, adding salient poles also has some effects to the torque ripple of the motor. Therefore, in selecting the ratio of l_{slt} to the l_{stk} , torque ripple needs to be considered, and it can be calculated by using formula shown in Eq. (4). The torque comparison of the three models are shown in Fig. 15.

$$T_{ripple} = \frac{T_{max} - T_{min}}{T_{avg}} \quad (4)$$

Fig. 14 shows that each model has slightly different

Table 1. Torque characteristics comparison

Parameters	Saliency [%]		
	40%	20%	10%
Average continuous torque [N.m]	0.502	0.501	0.503
Starting torque [N.m]	0.481	0.393	0.337
Minimum torque [N.m]	0.103	0.114	0.133
Maximum torque [N.m]	0.948	0.946	0.956
Connecting torque [N.m]	0.2344	0.300	0.306
Torque ripple [%]	168.33	166.07	163.62

Table 2. Performance comparison

Parameter	Universal motor	Proposed HSRM
Length of stator	95	78
Width of stator	72	58
Output power(W)	576	753
Rated speed (rpm)	13,740	18,000
Rated torque (Nm)	0.4	←
Air gap (mm)	0.3	0.5 – 1.2
Efficiency	63	70

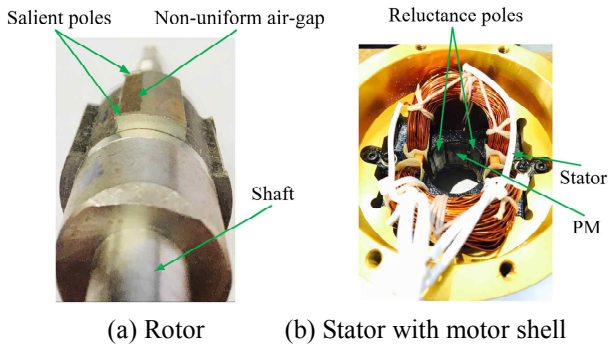


Fig. 15. Prototype of proposed motor

torque profile and the second model with 20% saliency has the lowest torque ripple compared to others, thus it is selected for manufacture. The numerical comparison between the models is shown in Table 1.

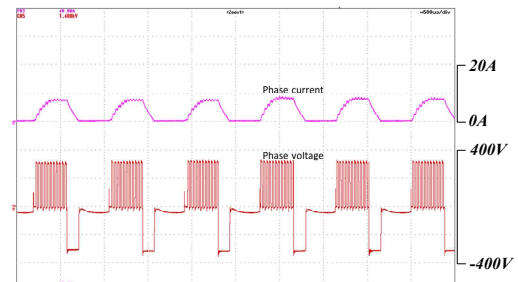
4. Experiment Results

To verify the proposed design, a prototype of hybrid SRM has been manufactured, which is shown in Fig. 15. Some of the main dimensions and specifications of the motor are given in the appendix. The motor control involves voltage chopping control that is used because of its simplicity. The power switches are turned on and off accordingly to allow enough current to flow depending on the needed speed and torque. The experimental result is shown in Fig. 16. It can be seen in the figure that the voltage waveform shows the switching form which happens in the control strategy. The motor is operated in no-load and load condition at the rated speed. Unlike universal motor which speed decreases if load is given, the proposed motor is able to maintain the speed while delivering the required torque. The comparison of universal motor and the proposed HSRM is shown in Table 2.

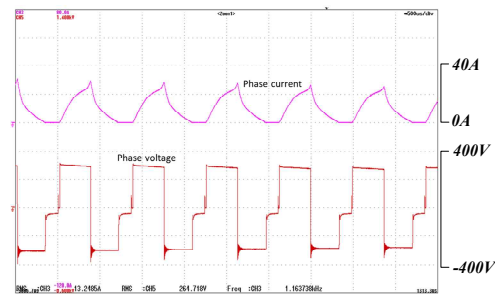
5. Conclusion

This paper deals with the design and analysis of a hybrid 4/4 poles switched reluctance motor to replace the conventional universal motor in a commercial blender.

The proposed motor has high starting torque to blend hard food or ice and is able to self-start in unidirectional



(a) No-load test torque = 0.1[Nm] and speed = 18000[RPM]



(b) Load torque = 0.4[Nm] and speed = 18000[RPM]

Fig. 16. Experiment result of the proposed motor

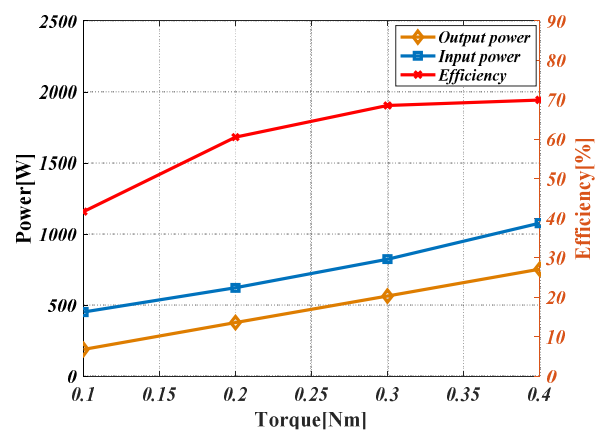


Fig. 17. Efficiency of proposed motor

direction. Non-uniform air-gap to modify torque profile is achieved by modifying rotor structure. Salient poles on both rotor edges were implemented. The saliency value is optimized to further decrease torque ripple. Other than being low cost, the proposed motor is able to deliver the

require torque for load, regardless of rotating speed. The efficiency of the proposed motor by experiment is shown in Fig. 17. Simulations and experiments show the viability of the proposed motor in blender application.

Appendix

Table 3. Motor dimensions

Parameters	Value
Number of stator pole	4
Number of rotor pole	4
Length of stator (mm)	78
Stack length (mm)	30
Air-gap (mm)	0.5-1.2

Acknowledgment

This research was supported by Basic Science Research Program through the National Research Foundation of Korea(NRF) funded by the Ministry of Education (2018 R1D1A1B07043735) and by Kyungsoong University Grants in 2018.

References

- [1] T.J.E Miller, "Switched Reluctance Motor and Their Control," *Magna Physics Publishing*, Aug 1, 1993
- [2] M. Ikeda, S. Sakabe, and K. Higashi, "Experimental study of high speed induction motor varying rotor core construction," *IEEE Transactions on Energy Conversion*, vol. 5, no. 1, pp. 98-103, March 1990.
- [3] N. Bianchi, S. Bolognani, and F. Luise, "High speed drive using a slotless PM motor," *IEEE Transactions on Power Electronics*, vol. 21, no. 4, pp. 1083-1090, July 2006.
- [4] R. Krishnan, "Switched Reluctance Motor: Modeling, Simulation, Analysis, Design, and Applications," *CRC Press*, 2001.
- [5] D. H. Lee, T. H. Pham and J. W. Ahn, "Design and operation characteristics of four-two pole high-speed SRM for torque ripple reduction," *IEEE Transactions on Industry Electronics*, vol. 60, no. 9, pp. 3637-3643, September 2013.
- [6] K. Lu, P.O. Rasmussen, S.J. Watkins and F. Blaabjerg, "A new low-cost hybrid switched reluctance motor for adjustable-speed pump applications," *IEEE Transaction on Industry Application*, vol. 47, no. 1, pp. 314-321, January /February 2011.
- [7] K. Lu, U. Jakobsen and P. O. Rasmussen, "Single-phase hybrid switched reluctance motor for low-power low-cost applications," *IEEE Transactions on Magnets*, vol. 47, no. 10, October 2011.
- [8] V. Torok, U.S. patent, No. 5345131, September 6, 1994.
- [9] V. Torok, U.S. patent, No. 6204587, March 20, 2001.
- [10] V. Torok and K. Loreth, "The world's simplest motor for variable speed control? The Cyrano motor, a PM-biased SR-motor of high torque density," in *Proceedings of 5th European Conference on Power Electronics and Applications*, vol. 6, pp. 44-48, Sep. 13-16, 1993.



Kwang-Il Jeong was born in Jinju, Korea in 1986. He received his B.S. degree in Mechatronics Engineering from Gyeongnam National University of Science and Technology, Jinju, Korea, in 2009, and M.S. degree in Kyungsoong University, Busan, Korea, in 2012. Now, he is studying in Kyungsoong University, Busan, Korea as a Ph.D. student in the Department of Mechatronics Engineering. His research interests are motor design and control.



Jin-Woo Ahn was born in Busan, Korea, in 1958. He received his B.S., M.S., and Ph.D. degrees in Electrical Engineering from Pusan National University, Busan, Korea, in 1984, 1986 and 1992, respectively. He has been with Kyungsoong University, Busan, Korea, as a professor in the School of Mechanical & Mechatronics Engineering since 1992. He is the director of the Smart Mechatronics Advanced Research and Technology Institute and Senior Easy Life RIS Center and was Vice President of KIEE. He is the author of five books including SRM, the author of more than 200 papers and has more than 30 patents. His current research interests are advanced motor drive systems and electric vehicle drives. He also received many awards from IEEE, KIEE and KIPE and Government including Order of Science and Technology Merit from the President of the Republic of Korea for his numerous contributions for the electrical engineering. He served as a Conference Chairman of International Conference on Electric Machines and Systems 2013(ICEMS2013), International Conference on Industrial Technology 2014 (IEEE/ICIT2014) and IEEE Transportation Electrification Conference and Expo 2016 Busan (ITEC2016 Busan). He serves as a Chairman of International Steering Committee of ICEMS2018 Jeju and Conference Chairman of IEEE Transportation Electrification Conference and Expo 2019 Jeju(ITEC2019 Jeju). He is a Fellow of the Korean Institute of Electrical Engineers, a member of the Korean Institute of Power Electronics and a Senior member of the IEEE.